APPLIED PHYSICS LETTERS **103**, 233114 (2013)

Ultrafast spectroscopy of super high frequency mechanical modes of doubly clamped beams

Oliver Ristow,[1] Moritz Merklein,[1] Martin Grossmann,[1] Mike Hettich,[1] Martin Schubert,[1] Axel Bruchhausen,[1,a)] Jochen Grebing,[2] Artur Erbe,[2] Denis Mounier,[3] Vitalyi Gusev,[4] Elke Scheer,[1] Thomas Dekorsy,[1] and Elaine C. S. Barretto[1,b)]

[1]*Department of Physics and Center of Applied Photonics, University of Konstanz, D-78457 Konstanz, Germany*

[2]*Helmholtz-Zentrum Dresden - Rossendorf, Institute of Ion-Beam Physics and Materials Research, D-01328 Dresden, Germany*

[3]*IMMM, UMR-CNRS 6283, ENSIM, PRES UNAM, Université du Maine, 72085 Le Mans, France*

[4]*LAUM, UMR-CNRS 6613, PRES UNAM, Université du Maine, 72085 Le Mans, France*

(Received 14 July 2013; accepted 20 November 2013; published online 6 December 2013)

We use ultrafast pump-probe spectroscopy to study the mechanical vibrations in the time domain of doubly clamped silicon nitride beams. Beams with two different clamping conditions are investigated. Finite element method calculations are performed to analyse the mode spectra of both structures. By calculating the strain integral on the surface of the resonators, we are able to reproduce the effect of the detection mechanism and identify all the measured modes. We show that our spectroscopy technique combined with our modelling tools allow the investigation of several different modes in the super high frequency range (3-30 GHz) and above, bringing more information about the vibration modes of nanomechanical resonators. © *2013 Author(s). All article content, except where otherwise noted, is licensed under a Creative Commons Attribution 3.0 Unported License.* [http://dx.doi.org/10.1063/1.4844775]

Nanomechanical systems have been intensively studied in the recent years.[1,2] Particularly, systems such as cantilevers and doubly clamped beams have been widely used in a range of applications, from sensing[3] to optomechanics[4] and even quantum ground state cooling.[5] Some of the most common measurement techniques are based on electrical[1,2,6–8] or optical excitation by means of (modulated) continuous wave (CW) laser light.[9,10] In both cases, the readout is mostly accomplished electrically or by interferometry, and investigations have concentrated on the MHz frequency range, while a few examples of fundamental modes in the low GHz range have been reported.[11–14]

In parallel, the field of pump-probe spectroscopy and laser-based ultrasonics has progressed. Recent developments enable to access the acoustic dynamics of single nanostructures.[15–17] It has also been shown that the vibrational spectra of these nanostructures can strongly depend on the coupling to the substrate.[18–20] Using these methods, mechanical modes in the GHz to THz frequency range can be observed in the time domain. Earlier work demonstrated the capability to excite high frequency acoustic modes in nm-thin membranes[21,22] and other planar acoustic resonators.[23,24] We are extending the investigations of laser-based ultrasonics to the super high frequency modes of beam resonators.

Clamping conditions in beams have been theoretically studied for several cases, such as non-ideal clamping,[25] simply supported and sliding conditions,[26] or even partly clamped nanotubes.[27] Experimentally, it has also been shown that the support compliance plays a role in the performance of micromechanical devices.[28] Here, by laying the beam on the substrate, a condition of full bottom support is obtained and investigated, numerically and experimentally, and compared with the free standing condition. The numerical analysis is performed using 3D finite element method (Comsol Multiphysics software), and the geometry of the simulated structures reproduces the dimensions of the fabricated ones: 2.5 μm length, 170 nm width, 107 nm silicon nitride thickness, and 20 nm top gold layer. Both geometries have zero displacement condition assigned to the sides of the beam, representing the support of the pads. In the case of the fully supported beam, the bottom boundary has also been fixed, while for the free standing beam all the other boundaries are mechanically free. By performing an eigenfrequency analysis, the expected frequencies for the vibration modes of both types of beams were calculated and are presented in Fig. 1 for a range of mode numbers, with mode number 1 representing the fundamental mode order. The modes are assigned as a_n for the free standing beam and b_n for the supported beam, n being the order in which they appear in frequency and therefore not meaning that they represent the same mode for both beams. This plot was constructed by assigning a frequency value to each mode number and subsequently connecting these values by lines. The curves end at the cut-off frequency of the modes. From a standing wave point of view, the data shown in Fig. 1 are strictly true only for integer mode orders. However, the figure can also be interpreted as a dispersion diagram for wave propagation in an infinite beam when the wavelength is equal to two times the length of the beam divided by the mode order.[29] The curves clearly show that the mode spectra are strongly affected by the extra clamping condition, and especially that the first modes of the supported beam start at much higher frequencies than in the case of the free standing beam,

a)Also at IB&CAB-CONICET, Bariloche, Argentina.
b)Electronic mail: elaine.barretto@uni-konstanz.de

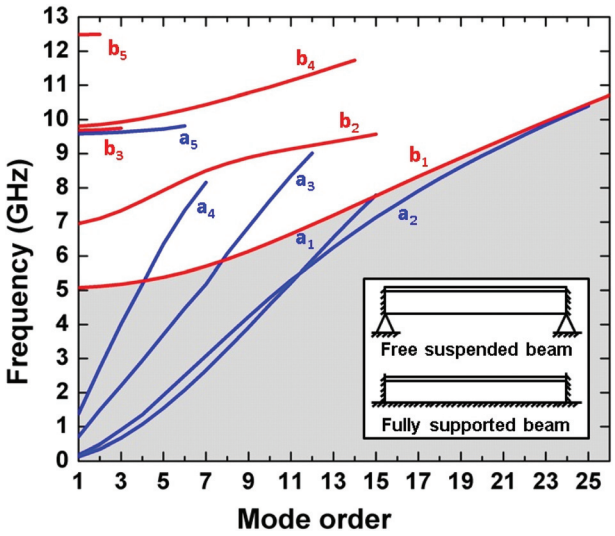

FIG. 1. Numerically calculated vibration frequencies for the modes of a free standing beam (a_n, blue lines) and a fully supported beam (b_n, red lines) with the same dimensions (2.5 μm length, 170 nm width, silicon nitride thickness 107 nm and 20 nm top gold layer). Both beams are clamped on the long ends. The grey shaded area indicates the frequencies that lay below the first mode of the fully supported beam. The inset shows a schematic drawing representing the clamping conditions of the two beams.

as marked by the grey shaded area in Fig. 1. It is known that in plates rigidly attached to the substrates a lower bound exists for the propagating waveguide modes,[30,31] which coincide with the frequencies of the acoustic resonances for the waves propagating normally to plate faces, while the modes with arbitrary low frequencies do not propagate. Experimentally, this means that it would be difficult for current conventional electrical/ magnetic techniques to detect any modes in supported beams with these dimensions. To verify which of those modes can be measured by pump-probe spectroscopy and study the differences between them, we produced samples of the two different types of beams.

The beam structures are fabricated using electron beam lithography (EBL), followed by dry and wet etching steps. The samples are produced from a commercial silicon wafer with 400 nm thermal silica and a top layer of 107 nm silicon nitride with a high tensile internal stress of 1.39 GPa. This high stress was chosen in order to improve the mechanical stability and to increase resonance frequencies as well as quality factors of the beam structures.[32]

EBL is used to define the beams with the dimensions previously described in PMMA 950 K resist. A very thin layer of chromium (used for adhesion purposes) and a 20 nm thick gold film are thermally evaporated, followed by a lift-off process. The remaining gold serves as an etch mask during the reactive ion etching process and later as an optical transducer in the experiment. Hydrofluoric acid (HF) is used to remove parts of the SiO_2 layer, releasing the beam (see Fig. 2(a)), which is then suspended 400 nm above the silicon substrate and clamped between two squared pads that sit on SiO_2 pedestals. A second sample with the same beams is additionally etched in HF for removal of the SiO_2 pedestals, allowing the beam to softly land on the silicon substrate (see Fig. 2(b)).

All measurements are performed using a high speed asynchronous optical sampling setup.[33] Two Ti:sapphire ring

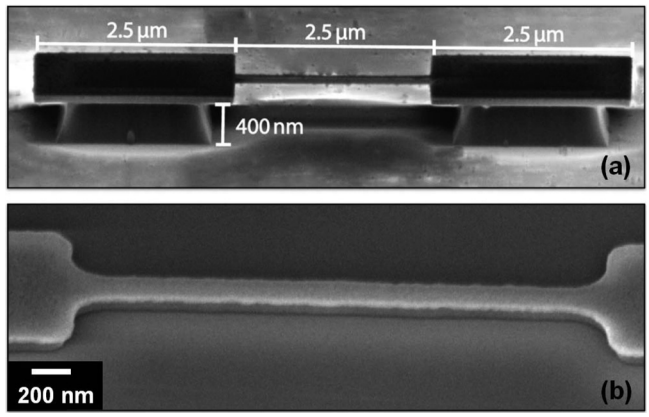

FIG. 2. Scanning electron micrographs of (a) free standing beam with 400 nm silica pedestals and (b) fully supported beam laying directly on the silicon substrate.

cavity lasers with a repetition rate of 800 MHz are asynchronously linked to each other with a fixed repetition rate offset of 5 kHz. This offset is actively stabilized and introduces a linearly increasing time delay between the pump and the probe pulse, enabling a scanning of the measurement window of 1.25 ns without mechanical delay line and with femtosecond time resolution.[34] The time resolved change in reflectivity of the nanostructure is directly recorded using a 125 MHz photo-detector without using an extra modulation technique. It is worth mentioning that while other measurement techniques (such as electrical ones) are limited to lower frequencies, the technique here described is limited to high frequencies (above ~2 GHz) due to the measurement window.

In order to address a single nanostructure, the pump and probe pulses are focused below 2 μm spot size by means of a microscope objective, which also collects the reflected light from the sample. The collinear beam path in the microscope is achieved using polarizing beam splitter cubes. By cross-polarizing pump and probe light, the reflected pump light can be filtered out. The measurements were performed using 15 mW pump power at 790 nm wavelength and 1.75 mW probe power at 820 nm central wavelength.

Figure 3 shows the time domain reflectivity changes $\Delta R/R$ obtained for both types of beams with same dimensions.

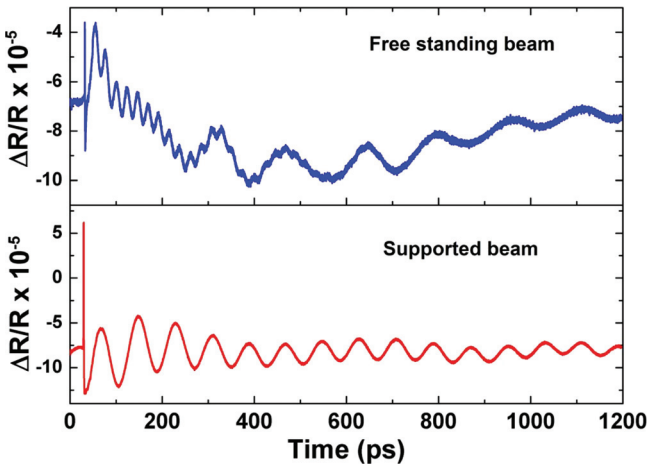

FIG. 3. Time-domain reflectivity changes obtained experimentally for the free standing beam (top) and the supported beam (bottom).

At zero time delay between pump and probe, a sharp and pronounced rise in ΔR/R is observed, caused by the absorption of the pump pulse in the gold layer, which results in a rapid heating of the electron gas, inducing a strong change in the dielectric function and thus in ΔR/R.[35] The heated electron gas then thermalizes with the lattice in the gold film, resulting in an impulsive thermal stress therein.[36] This thermal stress excites the observed system of vibrational modes. The time traces of the free standing beam shows a superposition of one higher and several lower frequency oscillations, while the spectrum of the supported beam is simpler, with a few lower frequency oscillations. By subtracting the electronic background from the time spectra, the vibrational contributions can be extracted. Figure 4(a) shows the frequency spectra obtained from numerical fast Fourier transforms (FFT) of the time oscillations of the free standing (blue, full line) and the supported beam (red, dotted line). As expected from the time traces, the FFT of the free standing beam shows several peaks, with frequencies of approximately 2 GHz, 6 GHz, 9 GHz, 12.5 GHz, and 43 GHz; while the supported beam shows only two: a strong peak at 12.7 GHz and a weaker one at 9.8 GHz.

The dispersion curves presented in Fig. 1 are rather complex, which makes a direct comparison with the measurements difficult. It is therefore important at this point to include some contribution of the laser detection process in the calculations, since not all the modes presented in Fig. 1 can be efficiently detected by the spectroscopy technique here applied. In reflectivity measurements, the detection is most sensitive to the changes in the refractive index which are mainly caused by strain.[35] The strain distribution is very different for each of the vibration modes, and it is expected that modes that present nearly equal amounts of positive and negative strain will not be detected due to counteraction. A way to quantify this in the modeling can be by numerically integrating the strain of the modes in a certain area of the beam corresponding to the detection area. Since the probe laser spot diameter has nearly the same dimensions as the beam length, it is a reasonable approximation to assume a uniform excitation/detection throughout the whole beam surface. We therefore integrate the volumetric strain (sum of the diagonal elements of the strain matrix) over the gold surface of the whole beam and normalize it by the maximum volumetric strain amplitude in the same area, for both types of beams. The results of these calculations are shown in Fig. 4(b), with blue circles representing the free standing beam and red squares representing the supported beam. Each of the points corresponds to a mode number in Fig. 1, and the modes corresponding to the highest values are marked accordingly: a_5 in the case of the free standing beam, and b_3 and b_5 for the supported beam. The distribution of the total displacement for these three modes in a cross section taken in the middle of the beam is plotted in Fig. 4(c). The shape of the three assigned modes in Fig. 4(c) also indicates that they have the same nature (symmetric across the width of the beam and "breathing" movement of the edges). The experimentally detected vibration frequency of 12.7 GHz corresponds to half wavelength resonance of the mode propagating along the beam of 2.5 μm length with the phase velocity of 62.5 km/s. This velocity is much higher than the velocities of the lowest in frequency modes allowed in the free standing beams. For comparison, the flexural mode resonances of the free standing beams clamped at one end are just approaching the GHz frequency range when the beams are shorter than 0.5 μm.[13]

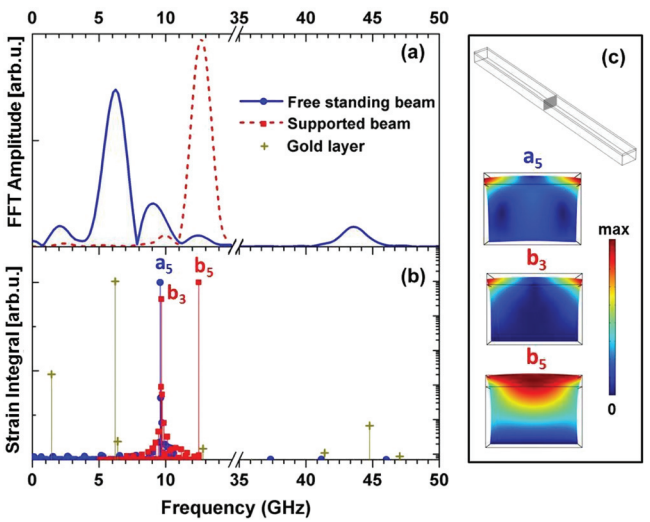

FIG. 4. (a) Frequency spectra obtained from the Fourier transformation of the experimental time traces. (b) Numerical results of the normalized integral of the strain on the surface of the gold layer for the two types of beams and for a released gold layer; the break in the frequency axis is a region that presents no peaks in the experimental or numerical results. (c) Cross section of the distribution of the total displacement of three different modes of the beams.

For every peak in the strain integral calculations, a corresponding peak in the frequency spectra in Fig. 4(a) can be seen. To be able to assign the remaining peaks in the experimental spectra, we additionally performed the strain integral calculations for a gold layer mechanically detached from the beam, to account for changes in the adhesion properties between the metal layer and the nitride that might occur after the laser irradiation.[37–39] The calculations of the strain in the gold layer are also shown in Fig. 4(b), represented by dark yellow crosses. Once more, an excellent agreement is achieved, such that all the remaining modes of the free standing beam can be assigned to vibrations localized in the free gold layer. Naturally, this is a simplistic approximation, since the modes of the beam system and of the metal layer can be measured simultaneously, and that indicates that the metal layer is not completely detached, such that the bond even when soft is enough to couple the vibrations. Those metal modes are not as strongly present in the spectrum of the supported beam, showing that the effects of the laser on the gold adhesion are not so severe in this case, probably due to the thermal contact with the substrate.

In summary, we have investigated the vibration modes of nanomechanical beam resonators in the super high frequency range by ultrafast pump-probe spectroscopy, showing that this technique is powerful for the study of resonators with very small dimensions. Beams with two different clamping conditions were investigated, and the differences in their spectrum could be fully explained by our numerical model. Compared to standard techniques used in the characterization of nanomechanical resonators, this technique allows the detection of other vibration modes than the

flexural, and modes at much higher frequencies, helping also to understand the influence of clamping conditions and metallization and possibly more complex multi-layered systems.

This work was supported by the DFG (Deutsche Forschungsgemeinschaft) through the SFB 767 and by the Ministry of Science, Research and Arts of Baden Württemberg (Germany). We would like to thank Paul Leiderer and Peter Nielaba for the valuable discussions. A.B. acknowledges the fellowship of the A. von Humboldt Foundation. The work of V.G. was supported by the Humboldt-Gay Lussac award from the A. von Humboldt Foundation.

[1]K. L. Ekinci and M. L. Roukes, Rev. Sci. Instrum. **76**, 61101 (2005).
[2]A. N. Cleland, *Foundations of Nanomechanics*, 1st ed. (Springer-Verlag, New York, 2003).
[3]M. Li, H. X. Tang, and M. L. Roukes, Nat. Nanotechnol. **2**, 114–120 (2007).
[4]G. Anetsberger, O. Arcizet, Q. P. Unterreithmeier, R. Rivière, A. Schliesser, E. M. Weig, J. P. Kotthaus, and T. J. Kippenberg, Nat. Phys. **5**, 909–914 (2009).
[5]A. D. O'Connell, M. Hofheinz, M. Ansmann, R. C. Bialczak, M. Lenander, E. Lucero, M. Neeley, D. Sank, H. Wang, M. Weides, J. Wenner, J. M. Martinis, and A. N. Cleland, Nature **464**, 697–703 (2010).
[6]Q. P. Unterreithmeier, T. Faust, and J. P. Kotthaus, Phys. Rev. Lett. **105**, 27205 (2010).
[7]T. Rocheleau, T. Ndukum, C. Macklin, J. B. Hertzberg, A. A. Clerk, and K. C. Schwab, Nature **463**, 72–75 (2010).
[8]Q. P. Unterreithmeier, E. M. Weig, and J. P. Kotthaus, Nature **458**, 1001–1004 (2009).
[9]A. Sampathkumar, T. W. Murray, and K. L. Ekinci, Appl. Phys. Lett. **88**, 223104 (2006).
[10]B. Ilic, S. Krylov, and H. G. Craighead, J. Appl. Phys. **107**, 34311 (2010).
[11]H. X. M. Huang, C. A. Zorman, M. Mehregany, and M. L. Roukes, Nature **421**, 496 (2003).
[12]A. Gaidarzhy, G. Zolfagharkhani, R. L. Badzey, and P. Mohanty, Appl. Phys. Lett. **86**, 254103 (2005).
[13]N. Liu, F. Giesen, M. Belov, J. Losby, J. Moroz, A. E. Fraser, G. McKinnon, T. J. Clement, V. Sauer, W. K. Hiebert, and M. R. Freeman, Nat. Nanotechnol. **3**, 715–719 (2008).
[14]X. Sun, J. Zheng, M. Poot, C. W. Wong, and H. X. Tang, Nano Lett. **12**, 2299–2305 (2012).
[15]A. Juvé, Vand Crut, M. B. M. Maioli, Pand Pellarin, N. Del Fatti, and F. Vallée, Nano Lett. **10**, 1853–1858 (2010).
[16]O. L. Muskens, N. Del Fatti, and F. Vallée, Nano Lett. **6**, 552–556 (2006).
[17]G. V. Hartland, Chem. Rev. **111**, 3858–3887 (2011).
[18]V. Kotaidis, T. Dekorsy, S. Ibrahimkutty, D. Issenmann, D. Khakhulin, and A. Plech, Phys. Rev. B **86**, 100101 (2012).
[19]Y. Guillet, B. Audoin, M. Ferrié, and S. Ravaine, Phys. Rev. B **86**, 35456 (2012).
[20]P. V. Ruijgrok, P. Zijlstra, A. L. Tchebotareva, and M. Orrit, Nano Lett. **12**, 1063–1069 (2012).
[21]A. Bruchhausen, R. Gebs, F. Hudert, D. Issenmann, G. Klatt, A. Bartels, O. Schecker, R. Waitz, A. Erbe, E. Scheer, J.-R. Huntzinger, A. Mlayah, and T. Dekorsy, Phys. Rev. Lett. **106**, 77401 (2011).
[22]J. Cuffe, O. Ristow, E. Chávez, A. Shchepetov, P.-O. Chapuis, F. Alzina, M. Hettich, M. Prunnila, J. Ahopelto, T. Dekorsy, and C. M. Sotomayor Torres, Phys. Rev. Lett. **110**, 095503 (2013).
[23]N. D. Lanzillotti-Kimura, A. Fainstein, B. Jusserand, and A. Lemaître, Phys. Rev. B **79**, 35404 (2009).
[24]A. Fainstein, N. D. Lanzillotti-Kimura, B. Jusserand, and B. Perrin, Phys. Rev. Lett. **110**, 037403 (2013).
[25]J. Lee, J. Mech. Sci. Technol. **27**, 297–303 (2013).
[26]J. Lee and W. Schultz, J. Sound Vib. **269**, 609–621 (2004).
[27]P. Pine, Y. E. Yaish, and J. Adler, J. Appl. Phys. **110**, 124311 (2011).
[28]M. Kobrinsky, E. Deutsch, and S. Senturia, J. Microelectromech. Syst. **9**, 361–369 (2000).
[29]N. G. Stephen, J. Sound Vib. **292**, 372–389 (2006).
[30]W. M. Ewing, W. S. Jardetsky, and F. Press, *Elastic Waves in Layered Media* (McGraw-Hill, New York, 1957).
[31]L. Boeckx, P. Leclaire, P. Khurana, C. Glorieux, W. Lauriks, and J. F. Allard, J. Acoust. Soc. Am. **117**, 545–554 (2005).
[32]S. S. Verbridge, J. M. Parpia, R. B. Reichenbach, L. M. Bellan, and H. G. Craighead, J. Appl. Phys. **99**, 124304 (2006).
[33]A. Bartels, R. Cerna, C. Kistner, A. Thoma, F. Hudert, C. Janke, and T. Dekorsy, Rev. Sci. Instrum. **78**, 035107 (2007).
[34]R. Gebs, G. Klatt, C. Janke, T. Dekorsy, and A. Bartels, Opt. Express **18**, 5974–5983 (2010).
[35]C. Thomsen, H. T. Grahn, H. J. Maris, and J. Tauc, Phys. Rev. B **34**, 4129–4138 (1986).
[36]C.-K. Sun, F. Vallée, L. H. Acioli, E. P. Ippen, and J. G. Fujimoto, Phys. Rev. B **50**, 15337–15348 (1994).
[37]F. Kneier, T. Geldhauser, E. Scheer, P. Leiderer, and J. Boneberg, Appl. Phys. A **110**, 321–327 (2013).
[38]E. Buks and M. Roukes, Phys. Rev. B **63**, 033402 (2001).
[39]T. Pezeril, N. Chigarev, D. Mounier, S. Gougeon, P. Ruello, J.-M. Breteau, P. Picart, and V. Gusev, Eur. Phys. J. Spec. Top. **153**, 207–210 (2008).